Electronic Supplementary Information

Variational quantum eigensolver simulations with the multireference unitary coupled cluster ansatz: a case study of the C_{2v} quasi-reaction pathway of beryllium insertion to H_2 molecule

Kenji Sugisaki,*[1,2,3] Takumi Kato,[4] Yuichiro Minato,[4] Koji Okuwaki,[5] and Yuji Mochizuki[5,6]

[1]*Department of Chemistry, Graduate School of Science, Osaka City University, 3-3-138 Sugimoto, Sumiyoshi-ku, Osaka 558-8585, Japan.*

[2]*JST PRESTO, 4-1-8 Honcho, Kawaguchi, Saitama 332-0012, Japan.*

[3]*Centre for Quantum Engineering, Research and Education (CQuERE), TCG Centres for Research and Education in Science and Technology (TCG-CREST), 16th Floor, Omega, BIPL Building, Blocks EP & GP, Sector V, Salt Lake, Kolkata 700091, India.*

[4]*Blueqat Inc. 2-24-12 Shibuya, Shibuya-ku, Tokyo 150-6139, Japan.*

[5]*Department of Chemistry, Faculty of Science, Rikkyo University, 3-34-1 Nishi-ikebukuro, Toshima-ku, Tokyo 171-8501, Japan.*

[6]*Institute of Industrial Science, The University of Tokyo, 4-6-1 Komaba, Meguro-ku, Tokyo 153-8505, Japan.*

* Corresponding author: sugisaki@osaka-cu.ac.jp

Table of Contents

1. Gaussian basis set used in the calculations of BeH_2

In this study, we used the following contracted Gaussian basis set[S1,S2] for the UCCSD simulations of BeH_2 systems.

```
Beryllium
   S       6
     1          1267.0700000000  0.00194000
     2           190.3560000000  0.01478600
     3            43.2959000000  0.07179500
     4            12.1442000000  0.23634800
     5             3.8092300000  0.47176300
     6             1.2684700000  0.35518300
   S       3
     1             5.6938800000 -0.02887600
     2             1.5556300000 -0.17756500
     3             0.1718550000  1.07163000
   S       1
     1             0.0571810000  1.00000000
   P       3
     1             5.6938800000  0.00483600
     2             1.5556300000  0.14404500
     3             0.1718550000  0.94969200

Hydrogen
   S       3
     1            19.2406000000  0.03282800
     2             2.8992000000  0.23120800
     3             0.6534000000  0.81723800
   S       1
     1             0.1776000000  1.00000000
```

2. The UCCSD and MR-UCCpGSD energies and wave functions of BeH_2 with initial (unoptimized) amplitudes

In this work, initial values of excitation amplitudes t_{ijab} and t_{ia} are prepared based on perturbation theory by using eqn (9)–(11) in the main text. The energy differences between the approximated and the full-CI wave functions and the square overlaps with the full-CI wave functions of BeH_2 calculated from the UCCSD ansatzes with initially prepared (unoptimized) and optimized excitation amplitudes are summarized in Table S1, and those from VQE-MR-UCCpGSD are given in Table S2.

Table S1 Deviation of the computed energy from the full-CI value and square overlap with the full-CI wave functions of BeH_2 calculated from VQE-UCCSD simulations.

Point	RHF		UCCSD (initial amp)		UCCSD (optimized)	
	ΔE /kcal mol^{-1}	$\lvert\langle\Psi\vert\Psi_{\text{full-CI}}\rangle\rvert^2$	ΔE /kcal mol^{-1}	$\lvert\langle\Psi\vert\Psi_{\text{full-CI}}\rangle\rvert^2$	ΔE /kcal mol^{-1}	$\lvert\langle\Psi\vert\Psi_{\text{full-CI}}\rangle\rvert^2$
A	23.537	0.9713	2.567	0.9954	0.263	0.9996
B	23.631	0.9719	2.497	0.9951	0.271	0.9996
C	29.103	0.9489	4.507	0.9860	0.436	0.9988
D	37.781	0.8781	8.498	0.9414	1.082[a]	0.9902[a]
E	51.286	0.5244	18.946	0.6095	7.360[a]	0.7833[a]
F	55.533	0.7994	13.851	0.9077	0.910[a]	0.9891[a]
G	46.733	0.8839	9.204	0.9684	0.224	0.9995
H	41.922	0.9030	7.522	0.9769	0.172	0.9996
I	41.105	0.9071	7.241	0.9794	0.085	0.9998
J	40.815	0.9079	7.173	0.9796	0.056	0.9998

[a]Taken from unconverged UCCSD simulations after 10000 iterations.

Table S2 Deviation of the computed energy from the full-CI value and square overlap with the full-CI wave functions of BeH_2 calculated from VQE-MR-UCCpGSD simulations.

Point	CASSCF(2e,2o)		MR-UCCpGSD (initial amp)		MR-UCCpGSD (after 10000 iterations)[a]	
	ΔE /kcal mol^{-1}	$\lvert\langle\Psi\vert\Psi_{\text{full-CI}}\rangle\rvert^2$	ΔE /kcal mol^{-1}	$\lvert\langle\Psi\vert\Psi_{\text{full-CI}}\rangle\rvert^2$	ΔE /kcal mol^{-1}	$\lvert\langle\Psi\vert\Psi_{\text{full-CI}}\rangle\rvert^2$
D	33.452	0.9227	8.660	0.9804	0.946	0.9923
E	40.378	0.8756	33.106	0.8837	2.143	0.9507
F	41.843	0.8848	25.561	0.9151	0.829	0.9972

[a]Taken from unconverged MR-UCCpGSD simulations after 10000 iterations.

3. Trotter term ordering dependence on the UCCSD/STO-3G energy of BeH_2 at point E

It is known that Trotterized UCC ansatz is not equivalent to the original (un-Trotterized) ansatz, and ordering of the excitation operators in the Trotter decomposition affects the energy expectation value.[S3] It should be noted that dependence of the term ordering in Trotterized UCC ansatz implies that optimal values of the variational parameter also depend on the ordering of terms in Trotterized UCC ansatz. To disclose the effect of Trotter term ordering on the VQE-UCCSD energies, we have examined ten numerical simulations with randomly shuffled term orderings in BeH_2 at point E, using STO-3G basis set. The ordering of terms is fixed during the VQE parameter optimizations, and other computational conditions such as optimization algorithm (COBYLA), initial excitation amplitudes (based on eqn (9) and (11) for t_{ijab} and t_{ia}, respectively) are fixed. The results of ten simulations are summarized in Table S3. The standard deviation for ten simulations is calculated to be 0.092 kcal mol^{-1}, which is sufficiently smaller than the averaged $\Delta E_{\mathrm{UCCSD-full\text{-}CI}}$ value (2.812 kcal mol^{-1}).

Table S3. The VQE-UCCSD/STO-3G simulation results of BeH_2 at point E, with randomly shuffled term ordering of cluster operators.

Trial	$\Delta E_{\mathrm{UCCSD-full\text{-}CI}}$/kcal mol^{-1}	$\lvert\langle\Psi_{\mathrm{UCCSD}}\vert\Psi_{\mathrm{full\text{-}CI}}\rangle\rvert^2$	Number of iterations
1	2.841	0.9616	3534
2	2.834	0.9648	4268
3	2.687	0.9705	4286
4	2.842	0.9645	3865
5	2.848	0.9626	3797
6	2.745	0.9656	3937
7	2.885	0.9609	4186
8	2.830	0.9647	4149
9	2.887	0.9613	3703
10	2.724	0.9679	4322

4. VQE-UCCSD/STO-3G simulations of LiH

In order to check the optimization algorithm dependences and the initial excitation amplitude dependences on the energies and convergence behaviour of the UCCSD ansatz, we have carried out VQE-UCCSD/STO-3G simulations of LiH molecule with interatom distances R(Li–H) = 1.0, 2.0, 3.0, and 4.0 Å. In the VQE simulations we examined three optimization algorithms, Nelder–Mead, Powell, and COBYLA. The quantum circuit simulations were performed with three different types of initial amplitudes for one-electron excitation operators, $t_{ia} = 0$, t_{ia}(unscaled) defined in eqn (10) in the main text, and t_{ia}(scaled) given in eqn (11) in the main text. The results for R(Li–H) = 1.0, 2.0, and 4.0 Å are summarized in Fig. S1–S3, respectively. The results for R(Li–H) = 3.0 Å are provided as Fig. 4 in the main text.

Nelder–Mead shows strong initial amplitude dependence, and it converges to local minima if zero amplitudes for one electron excitations ($t_{ia} = 0$) is employed. Even if t_{ia}(unscaled) is used, variational optimization sometimes stops before achieving the global minimum. These results exemplify importance of the choice of initial amplitudes for t_{ia} when the variational optimization is carried out by using Nelder–Mead algorithm.

By employing Powell and COBYLA algorithms, the VQE simulation converges to the global minimum regardless of the initial one-electron excitation amplitudes t_{ia} being adopted. The number of functional evaluations is larger than that in COBYLA. We concluded that COBYLA algorithm is the most plausible choice for the optimization algorithm among the three algorithms.

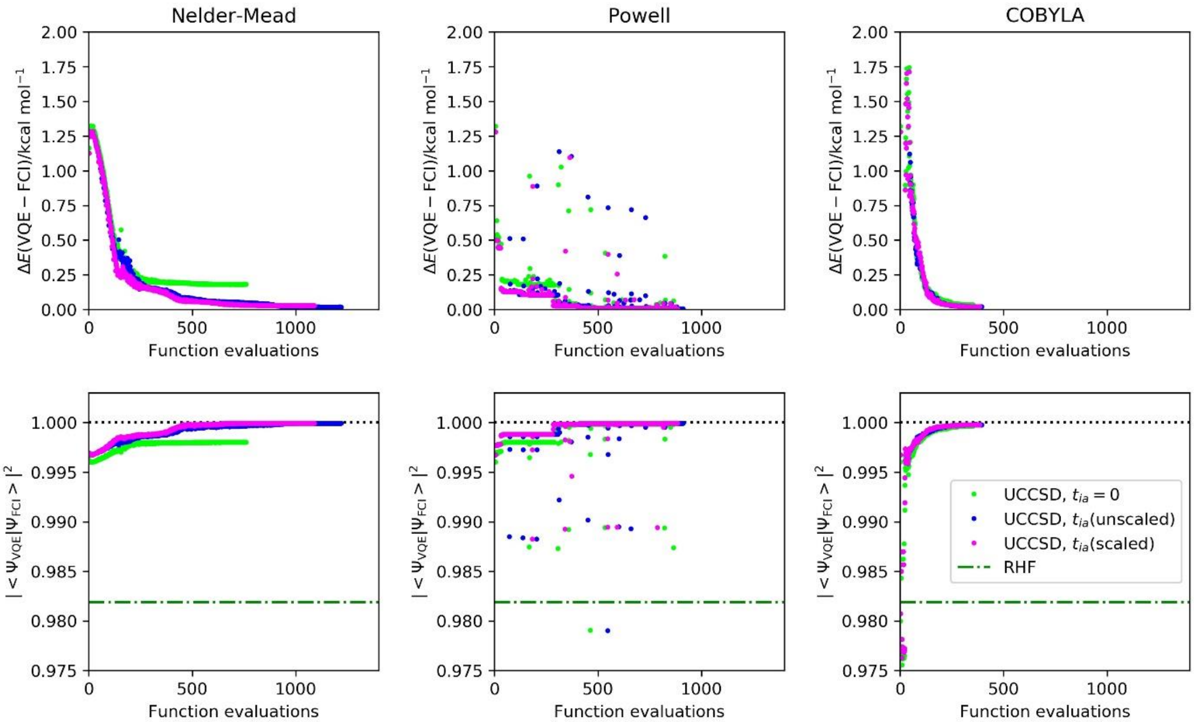

Fig. S1 The VQE-UCCSD simulation results of the LiH molecule with R(Li–H) = 1.0 Å.

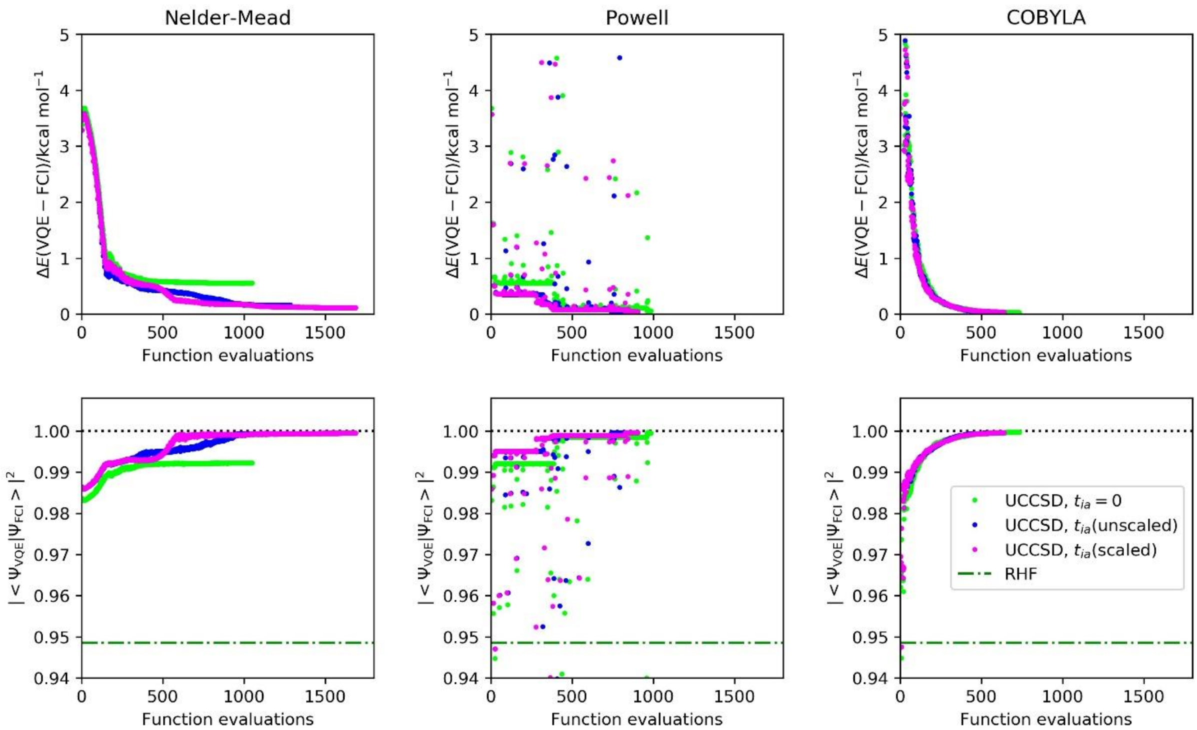

Fig. S2 The VQE-UCCSD simulation results of the LiH molecule with R(Li–H) = 2.0 Å.

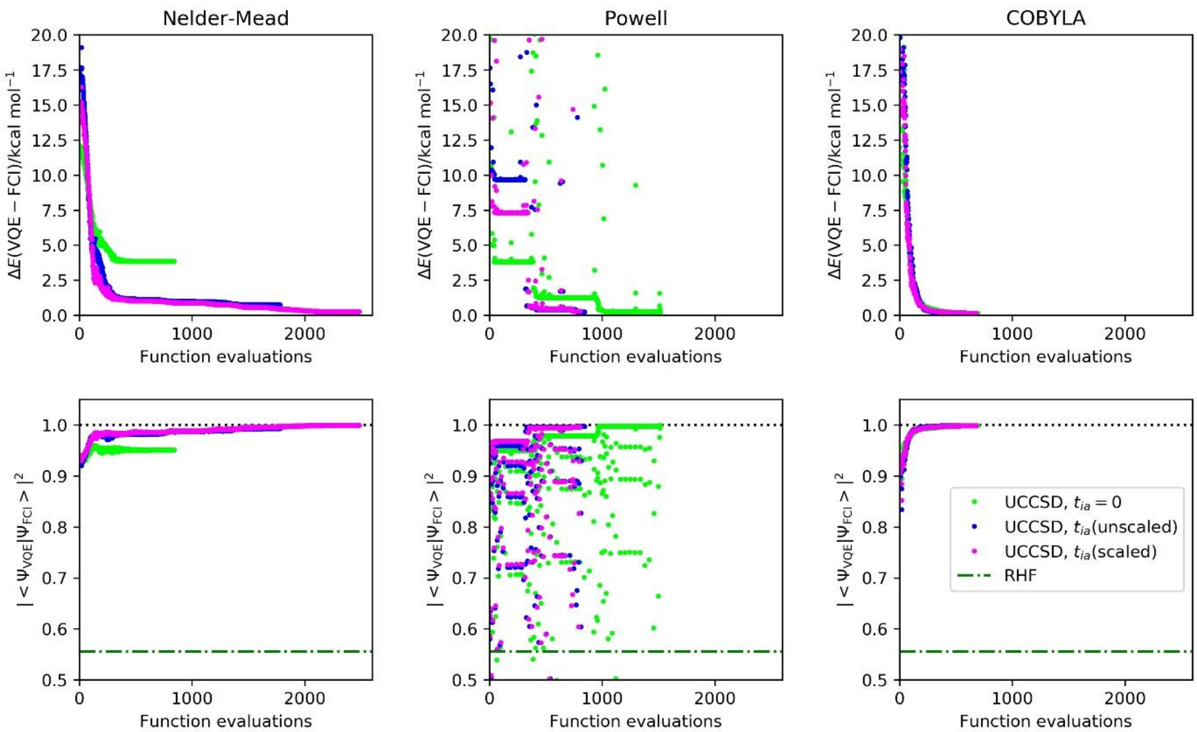

Fig. S3 The VQE-UCCSD simulation results of the LiH molecule with R(Li–H) = 4.0 Å.

5. Initial amplitude dependences on the UCCSD wave functions of BeH_2

Initial amplitude dependences on the UCCSD wave functions and energies of BeH_2 at points A, D, E, F, and I are plotted in Fig. S4. Similar to the VQE-UCCSD simulations of LiH molecule with COBYLA algorithm given in the rightmost of Fig. 4 in the main text and Fig. S1–S3, only small initial amplitude dependences were observed.

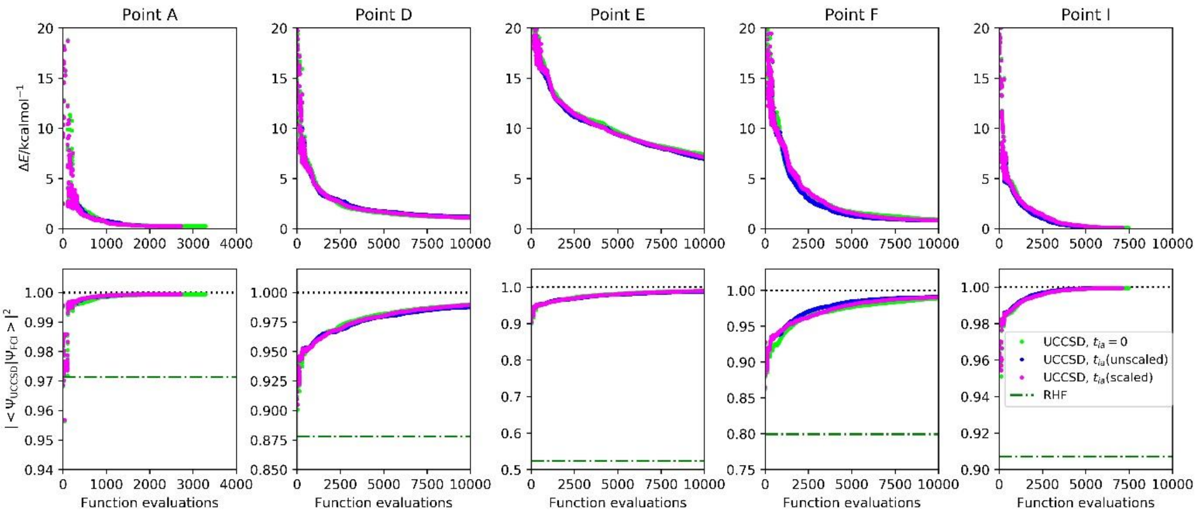

Fig. S4 Convergence behaviours of the VQE-UCCSD simulations of BeH_2 at points A, D, E, F, and I.

6. The RHF, CASSCF, UCCSD, MR-UCCpGSD, and full-CI energies of BeH_2

Table S4. Total energies of BeH_2 calculated at the RHF, CASSCF, UCCSD, MR-UCCpGSD, and full-CI level of theory.

Point	Energy/Hartree				
	RHF	CASSCF	UCCSD	MR-UCCpGSD	Full-CI
A	−15.74166329		−15.77875126		−15.77917109
B	−15.69956729		−15.73679352		−15.73722506
C	−15.62844195		−15.67412549		−15.67481986
D	−15.56267647	−15.56957424	−15.62115918[a]	−15.62137727[a]	−15.62288406
E	−15.52118967	−15.53857310	−15.59119125[a]	−15.59950447[a]	−15.60291972
F	−15.53646854	−15.55828427	−15.62351516[a]	−15.62364401[a]	−15.62496586
G	−15.61872113		−15.69283741		−15.69319416
H	−15.66988195		−15.73641384		−15.73668815
I	−15.69537506		−15.76074379		−15.76087998
J	−15.69786116		−15.76281423		−15.76290316

[a]Taken from unconverged simulations after 10000 iterations.

7. Singlet and triplet instabilities of the Hartree−Fock wave functions in BeH_2

The stability of the Hartree–Fock wave functions[S4] are examined for points D, E, and F of BeH_2. The calculations were performed by using Gaussian 16 (Revision B.01).[S5] The lowest three eigenvectors of points D, E, and F are listed below. At all the three points being investigated the spin-triplet B_2 state has the lowest, negative eigenvalue of the stability matrix, indicating presence of the triplet instability at these points. At point E the singlet B_2 state also has a negative eigenvalue. We also calculated the full-CI energy of the 1 $^1B_2$ state at point E, obtaining E = −15.64804984 Hartree.

```
Point D
 Eigenvector   1:      Triplet-B2   Eigenvalue=-0.0858502  <S**2>=2.000
       2 ->  7         0.16011
       3 ->  4         0.67065
       3 ->  6        -0.10016

 Eigenvector   2:      Singlet-B2   Eigenvalue= 0.0301214  <S**2>=0.000
       3 ->  4         0.70290

 Eigenvector   3:      Triplet-A1   Eigenvalue= 0.0373579  <S**2>=2.000
       2 ->  4         0.35694
       2 ->  8        -0.15021
       3 ->  7         0.57942

Point E
 Eigenvector   1:      Triplet-B2   Eigenvalue=-0.1261792  <S**2>=2.000
       2 ->  6         0.15521
       3 ->  4         0.67050
       3 ->  8        -0.11586

 Eigenvector   2:      Singlet-B2   Eigenvalue=-0.0025601  <S**2>=0.000
       3 ->  4         0.70338

 Eigenvector   3:      Triplet-A1   Eigenvalue= 0.0018909  <S**2>=2.000
       2 ->  4         0.29929
       2 ->  8        -0.15828
       3 ->  6         0.61206

Point F
 Eigenvector   1:      Triplet-B2   Eigenvalue=-0.1081938  <S**2>=2.000
```

```
      2 ->  4        -0.20130
      2 ->  6         0.12540
      3 ->  4         0.64022
      3 ->  6         0.17084

Eigenvector   2:      Triplet-B1   Eigenvalue=-0.0375084  &lt;S**2&gt;=2.000
      3 ->  5         0.70300

Eigenvector   3:      Triplet-B2   Eigenvalue= 0.0029764  &lt;S**2&gt;=2.000
      2 ->  4         0.53036
      2 ->  6        -0.10270
      3 ->  6         0.43681
```

8. Convergence behaviour of the VQE-UCCSD simulations in BeH_2

The difference between UCCSD and full-CI energies and the square overlap between UCCSD and full-CI wave functions are plotted in Fig. S5. The convergence is extremely slow for point E, although the variational optimizations converge rapidly for other geometries.

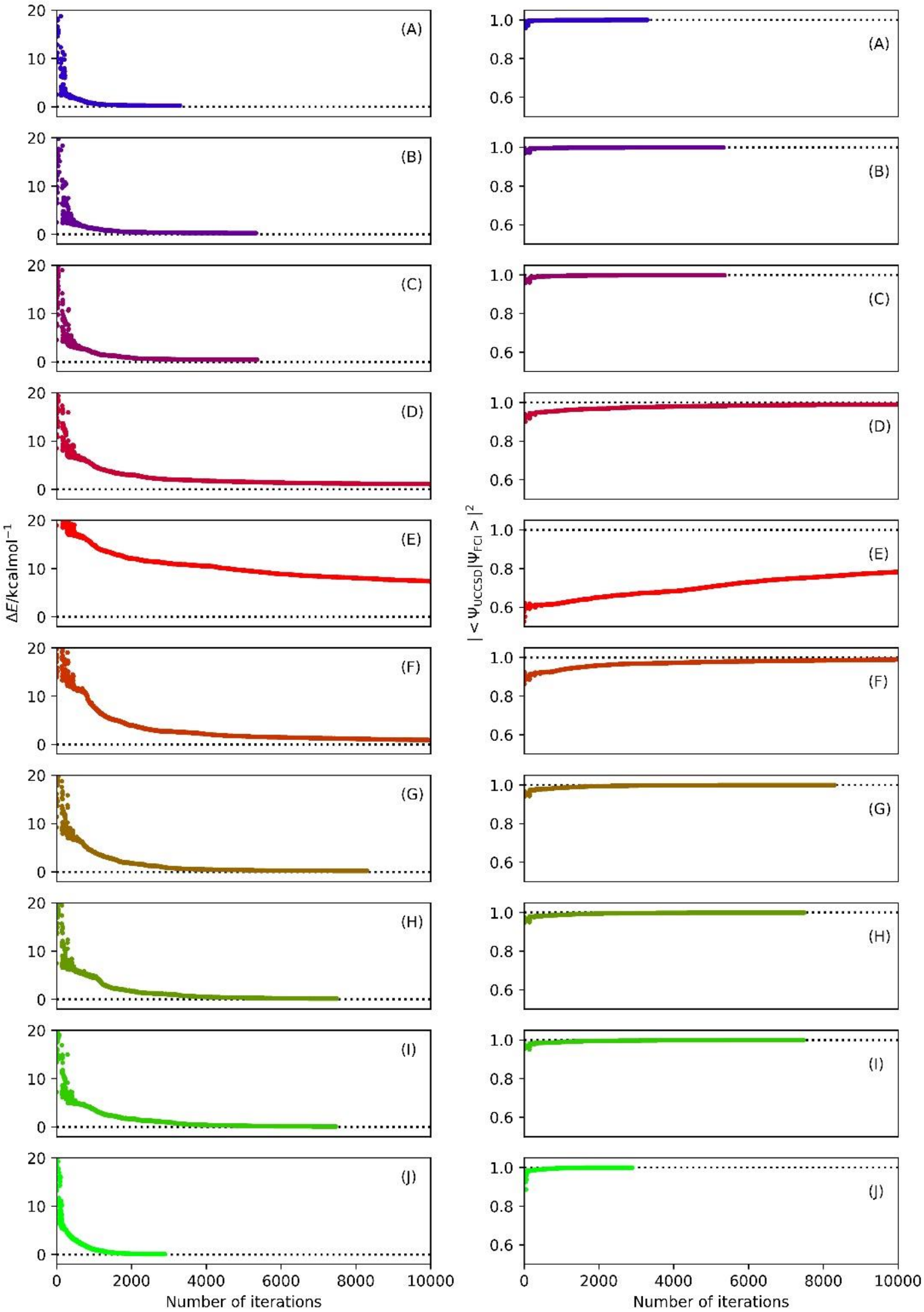

Fig. S5 Convergence behaviour of the VQE-UCCSD simulations. The difference between UCCSD and full-CI energies (left) and the square overlap between UCCSD and full-CI wave functions (right).

8. Fitting of the energy difference plots of BeH_2 at point E

Because numerical simulations of VQE at point E did not converge even after 10000 iterations, we have examined fitting the energy difference plots by using an exponential function $\Delta E = ax^b$, where x specify the iteration number. The results are plotted in Fig. S6. By using the data between 1000 and 10000 iterations, we can successfully be fitted by the convergence behaviour by the exponential function with a = 123.68 and b = −0.303 (UCCSD) and a = 1289.2 and b = −0.693 (MR-UCCpGSD). The fitted function is plotted in blue in Fig. S6.

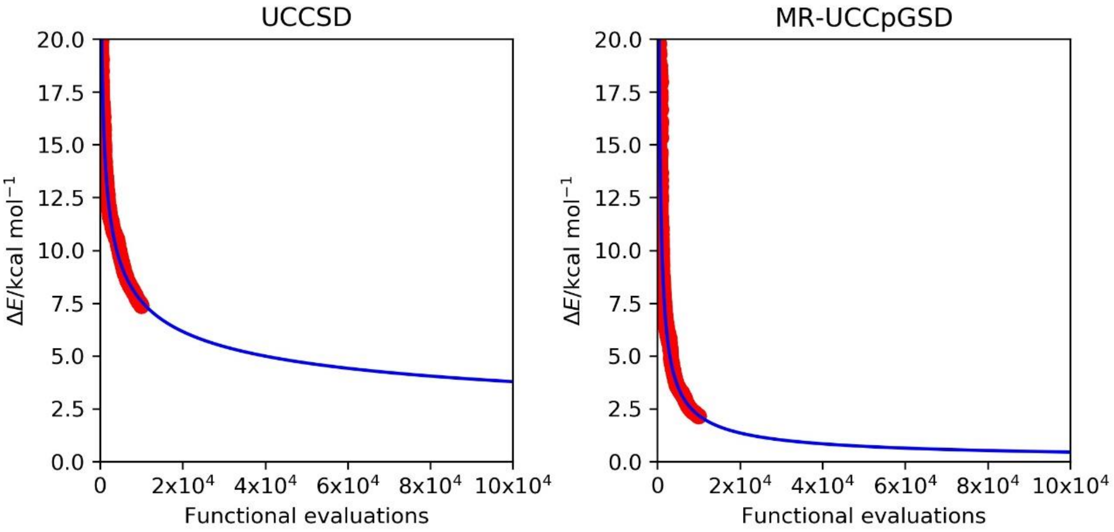

Fig. S6 The energy difference plots of BeH_2 at point E and the exponential function obtained by curve fitting.

9. The CCSD, CCSD(T), QCISD, and BD calculations of BeH_2 at points D, E, and F

To disclose complexity of the electronic structures at the geometry near avoided crossing in the Be + H_2 → BeH_2 reaction pathway, we carried out conventional CCSD, CCSD(T), QCISD, and Brueckner doubles (BD) calculations on classical computer by using Gaussian 09 (Revision B.01) software.[S6] Results of the quantum chemical calculations are summarized in Table S5.

At the CCSD level, we performed a T_1 diagnostic of Lee and Taylor.[S7] The T_1 diagnostic computes the Euclidian norm of the t_1 vector of the coupled cluster expansion normalized by the number of electrons included in the correlation procedure, which can be used to determine whether a single-reference-based electron correlation treatment is appropriate or not. According to the study by Lee and Taylor,[S7] multi-reference electron correlation procedure is more appropriate for larger T_1 value (e.g., > 0.02). The calculated T_1 diagnostic value is 0.0280, 0.0368, and 0.0222 for point D, E, and F, respectively, indicating inaccurate description of electronic structures at the HF level. The differences of the CCSD and CCSD(T) energies are calculated to be 0.000700, 0.004383, and 0.000567 Hartree for point D, E, and F, respectively. The large energy difference between CCSD and CCSD(T) implies importance of connected triple excitations from the HF reference.

We also calculated the energy difference between the average of QCISD and BD results and the CCSD energy defined in eqn (S1). The first difference between these methods occurs in the fifth-order perturbation theory, and departure of the ΔE(Handy) value defined in eqn (S1) from zero indicates importance of disconnected T_1 terms.[S8,S9]

$$\Delta E(\text{Handy}) = \frac{1}{2}\left(E_{\text{QCISD}} + E_{\text{BD}}\right) - E_{\text{CCSD}} \qquad \text{(S1)}$$

The ΔE(Handy) value is calculated to be −0.000030, −0.000011, and 0.000000 Hartree for point D, E, and F, respectively. This result also indicates non-negligible contributions of the T_1 terms at points D and E.

Table S5. The CCSD, CCSD(T), QCISD, and BD energies and the T_1 diagnostic values of BeH_2 at points D, E, and F.

Point	E_{CCSD} /Hartree	T_1 diagnostic	$E_{\text{CCSD(T)}}$ /Hartree	E_{QCISD} /Hartree	E_{BD} /Hartree
D	−15.62179120	0.0280	−15.62249082	−15.62200368	−15.62163786
E	−15.59734086	0.0368	−15.60172428	−15.59680810	−15.59789601
F	−15.62418998	0.0222	−15.62475691	−15.62422262	−15.62415806

10. The *k*-UpCCGSD/STO-3G simulations of BeH2 at point E

The *k*-UpCCGSD ansatz[S10,S11] is defined by eqn (S2).

$$|\Psi_{k-\mathrm{UpCCGSD}}\rangle = \prod_k \left(e^{T_k - T_k^\dagger}\right)|\Phi\rangle \tag{S2}$$

Here, $|\Phi\rangle$ is a reference wave function. The cluster operator is applied *k* times to the reference wave function, where each *k* factor has variationally independent amplitudes. T_k consists of fully generalized one-electron excitation operators as given in eqn (S4) and the generalized pair-double excitations as in eqn (S5). In this work, we assumed the dependence of the spin α–α and β–β transitions so as to $|\Psi_{k-\mathrm{UpCCGSD}}\rangle$ is spin symmetry-adapted. $T_k^\dagger$ is an adjoint of T_k, and it describes electron de-excitations from *u*-th orbital to the *v*-th orbital.

$$T_k = T_{1,k} + T_{2,k} \tag{S3}$$

$$T_{1,k} = \sum_{u\neq v} t_{uv}\left(a_{u\alpha}^\dagger a_{v\alpha} + a_{u\beta}^\dagger a_{v\beta}\right)/\sqrt{2} \tag{S4}$$

$$T_{2,k} = \sum_{u\neq v} t_{uuvv} a_{u\alpha}^\dagger a_{u\beta}^\dagger a_{v\beta} a_{v\alpha} \tag{S5}$$

Here, *u* and *v* are general molecular orbital indices. In the *k*-UpCCGSD ansatz, (occupied → occupied) and (unoccupied → unoccupied) excitations as well as (occupied → unoccupied) excitations in the reference wave function are considered.

In the *k*-UpCCGSD ansatz using VQE, it is difficult to estimate the initial amplitudes by means of perturbation theory. Thus, we started numerical simulations by setting all cluster amplitudes to zero. We carried out the *k*-UpCCGSD/STO-3G simulations with *k* = 1, 2, and 3, by using the HF and the CASSCF(2e,2o) orbitals as the reference.

Results of the VQE numerical simulations of BeH_2 at point E using *k*-UpCCGSD are summarized in Table S6. The simulations with the 3-UpCCGSD ansatz did not converge after 10000 iterations. According to our numerical simulations, the *k*-UpCCGSD ansatz with the CASSCF(2e,2o)/STO-3G reference orbital gave smaller ΔE value and larger square overlap with the full-CI wave function. The 3-UpCCGSD/STO-3G energies after 10000 iterations are higher than that of UCCSD (ΔE = 2.866 kcal mol^{-1}) and MR-UCCGSD (ΔE = 1.039 kcal mol^{-1}), but we cannot exclude the possibility that 3-UpCCGSD can give lower energy than the UCCSD and MR-UCCpGSD, by improving initial amplitudes or by taking more iterations.

Table S6. Results of the VQE simulations of BeH_2 at point E using *k*-UpCCGSD ansatz.

Reference orbitals	*k*	$\Delta E_{k\text{-UpCCGSD}-\text{full-CI}}$ /kcal mol^{-1}	$\lvert\langle\Psi_{k\text{-UpCCGSD}}\vert\Psi_{\text{full-CI}}\rangle\rvert^2$	Number of iterations
RHF	1	33.422	0.8037	2323
	2	30.133	0.8747	6991
	3	10.231[a]	0.8866[a]	10000
CASSCF	1	31.107	0.8768	2915
	2	31.037	0.8799	5371
	3	6.907[a]	0.9384[a]	10000

[a] The result from unconverged *k*-UpCCGSD simulation after 10000 iterations.

11. References

[S1] D. O'Neal, H. Taylor and J. Simons, Potential surface walking and reaction paths for C_{2v} Be + H_2 ← BeH_2 → Be + 2H ($^1A_1$). *J. Phys. Chem.,* 1984, **88**, 1510–1513.

[S2] G. D. Purvis III, R. Shepard, F. B. Brown and R. J. Bartlett, C_{2v} insertion pathway for BeH_2: A test problem for the coupled-cluster single and double excitation model. *Int. J. Quantum Chem.,* 1983, **23**, 835–845.

[S3] H. R. Grimsley, D. Claudino, S. E. Economou, E. Barnes and N. J. Mayhall, Is the Trotterized UCCSD ansatz chemically well-defined? *J. Chem. Theory Comput.,* 2020, **16**, 1–6.

[S4] T. Yamada and S. Hirata, Singlet and triplet instability theorems, *J. Chem. Phys.,* 2015, **143**, 114112.

[S5] M. J. Frisch, G. W. Trucks, H. B. Schlegel, G. E. Scuseria, M. A. Robb, J. R. Cheeseman, G. Scalmani, V. Barone, G. A. Petersson, H. Nakatsuji, X. Li, M. Caricato, A. V. Marenich, J. Bloino, B. G. Janesko, R. Gomperts, B. Mennucci, H. P. Hratchian, J. V. Ortiz, A. F. Izmaylov, J. L. Sonnenberg, D. Williams-Young, F. Ding, F. Lipparini, F. Egidi, J. Goings, B. Peng, A. Petrone, T. Henderson, D. Ranasinghe, V. G. Zakrzewski, J. Gao, N. Rega, G. Zheng, W. Liang, M. Hada, M. Ehara, K. Toyota, R. Fukuda, J. Hasegawa, M. Ishida, T. Nakajima, Y. Honda, O. Kitao, H. Nakai, T. Vreven, K. Throssell, J. A. Montgomery, Jr., J. E. Peralta, F. Ogliaro, M. J. Bearpark, J. J. Heyd, E. N. Brothers, K. N. Kudin, V. N. Staroverov, T. A. Keith, R. Kobayashi, J. Normand, K. Raghavachari, A. P. Rendell, J. C. Burant, S. S. Iyengar, J. Tomasi, M. Cossi, J. M. Millam, M. Klene, C. Adamo, R. Cammi, J. W. Ochterski, R. L. Martin, K. Morokuma, O. Farkas, J. B. Foresman and D. J. Fox, *Gaussian 16, Revision B.01*, Gaussian, Inc., Wallingford CT, 2016.

[S6] M. J. Frisch, G. W. Trucks, H. B. Schlegel, G. E. Scuseria, M. A. Robb, J. R. Cheeseman, G. Scalmani, V. Barone, B. Mennucci, G. A. Petersson, H. Nakatsuji, M. Caricato, X. Li, H. P. Hratchian, A. F. Izmaylov, J. Bloino, G. Zheng, J. L. Sonnenberg, M. Hada, M. Ehara, K. Toyota, R. Fukuda, J. Hasegawa, M. Ishida, T. Nakajima, Y. Honda, O. Kitao, H. Nakai, T. Vreven, J. A. Montgomery, Jr., J. E. Peralta, F. Ogliaro, M. Bearpark, J. J. Heyd, E. Brothers, K. N. Kudin, V. N. Staroverov, R. Kobayashi, J. Normand, K. Raghavachari, A. Rendell, J. C. Burant, S. S. Iyengar, J. Tomasi, M. Cossi, N. Rega, J. M. Millam, M. Klene, J. E. Knox, J. B. Cross, V. Bakken, C. Adamo, J. Jaramillo, R. Gomperts, R. E. Stratmann, O. Yazyev, A. J. Austin, R. Cammi, C. Pomelli, J. W. Ochterski, R. L. Martin, K. Morokuma, V. G. Zakrzewski, G. A. Voth, P. Salvador, J. J. Dannenberg, S. Dapprich, A. D. Daniels, Ö. Farkas, J. B. Foresman, J. V. Ortiz, J. Cioslowski and D. J. Fox, *Gaussian 09, Revision B.01*, Gaussian, Inc., Wallingford CT, 2009.

[S7] T. J. Lee and P. R. Taylor, A diagnostic for determining the quality of single-reference electron correlation methods. *Int. J. Quantum Chem., Quantum Chem. Symp.,* 1989, **S23**, 199–207.

[S8] N. C. Handy, J. A. Pople, M. Head-Gordon, K. Raghavachari and G. W. Trucks, Size-consistent Brueckner theory limited to double substitutions. *Chem. Phys. Lett.,* 1989, **164**, 185–192.

[S9] T. J. Lee, R. Kobayashi, N. C. Handy and R. D. Amos, Comparison of the Brueckner and coupled-cluster approaches to electron correlation. *J. Chem. Phys.,* 1992, **96**, 8931–8937.

[S10] J. Lee, W. J. Huggins, M. Head-Gordon and K. B. Whaley, Generalized unitary coupled cluster wave functions for quantum computation. *J. Chem. Theory Comput.,* 2019, **15**, 311–324.

[S11] G. Greene-Diniz and D. M. Ramo, Generalized unitary coupled cluster excitations for multireference molecular states optimized by the variational quantum eigensolver. *Int. J. Quantum Chem.,* 2021, **121**, e26352.